Biochimica et Biophysica Acta 1861 (2016) 108–118

Contents lists available at ScienceDirect

Biochimica et Biophysica Acta

journal homepage: www.elsevier.com/locate/bbalip

Replacement of two amino acids of 9*R*-dioxygenase-allene oxide synthase of *Aspergillus niger* inverts the chirality of the hydroperoxide and the allene oxide

Linda Sooman [a], Anneli Wennman [a], Mats Hamberg [b], Inga Hoffmann [a], Ernst H. Oliw [a,*]

[a] Division of Biochemical Pharmacology, Department of Pharmaceutical Biosciences, Uppsala University, Biomedical Center, SE-751 24 Uppsala, Sweden
[b] Department of Medical Biochemistry and Biophysics, Karolinska Institutet, SE-17177 Solna, Sweden

ARTICLE INFO

Article history:
Received 11 June 2015
Received in revised form 10 November 2015
Accepted 17 November 2015
Available online 18 November 2015

Keywords:
Fatty acid oxidation
Mass spectrometry
Class III cytochrome P450
Heme peroxidase
Linoleate diol synthase
Site-specific mutagenesis

ABSTRACT

The genome of *Aspergillus niger* codes for a fusion protein (EHA25900), which can be aligned with ~50% sequence identity to 9*S*-dioxygenase (DOX)-allene oxide synthase (AOS) of *Fusarium oxysporum*, homologues of the Fusarium and Colletotrichum complexes and with over 62% sequence identity to homologues of Aspergilli, including (DOX)-9*R*-AOS of *Aspergillus terreus*. The aims were to characterize the enzymatic activities of EHA25900 and to identify crucial amino acids for the stereospecificity. Recombinant EHA25900 oxidized 18:2*n*-6 sequentially to 9*R*-hydroperoxy-10(*E*),12(*Z*)-octadecadienoic acid (9*R*-HPODE) and to a 9*R*(10)-allene oxide. 9*S*- and 9*R*-DOX-AOS catalyze abstraction of the *pro-R* hydrogen at C-11, but the direction of oxygen insertion differs. A comparison between twelve 9-DOX domains of 9*S*- and 9*R*-DOX-AOS revealed conserved amino acid differences, which could contribute to the chirality of products. The Gly616Ile replacement of 9*R*-DOX-AOS (*A. niger*) increased the biosynthesis of 9*S*-HPODE and the 9*S*(10)-allene oxide, whereas the Phe627Leu replacement led to biosynthesis of 9*S*-HPODE and the 9*S*(10)-allene oxide as main products. The double mutant (Gly616Ile, Phe627Leu) formed over 90% of the 9*S* stereoisomer of HPODE. 9*S*-HPODE was formed by antarafacial hydrogen abstraction and oxygen insertion, i.e., the original H-abstraction was retained but the product chirality was altered. We conclude that 9*R*-DOX-AOS can be altered to 9*S*-DOX-AOS by replacement of two amino acids (Gly616Ile, Phe627Leu) in the DOX domain.

1. Introduction

Unsaturated fatty acids can be oxygenated to a large variety of biologically active metabolites by animals, plants, fungi and by some prokaryotes [1–4]. Their biosynthesis and physiological functions have been thoroughly investigated in humans. This led to the discovery of prostaglandins, leukotrienes and epoxy alcohols with key roles in reproduction, inflammation, fever, cancer development, and in formation of the skin water barrier [1,5]. In plants and fungi, these oxygenated fatty acids are designated oxylipins with regulatory functions in reproduction, development and in response to pathogens [2,6]. The growing numbers of sequenced plant and fungal genomes have led to discovery of gene families of putative enzymes involved in oxidation and further transformation of unsaturated fatty acids, *viz.*, lipoxygenases (LOX), fatty acid dioxygenases (DOX) of the peroxidase gene family, and cytochromes P450 (CYP). The task to experimentally link these putative enzymes to specific catalytic functions is facilitated by chemical synthesis of entire open reading frames, which can be used for expression of recombinant proteins. The published genome sequence data is generally correct, but the predicted intron–exon borders may need inspection.

Many fungi combine DOX and cytochromes P450 in DOX-CYP fusion enzymes, which belong to 6 different subfamilies (Fig. 1A), as judged from sequence homology and recombinant expression of enzymes of each subfamily. These enzymes oxidize fatty acids to diols, epoxyalcohols, and allene oxides without the need of an electron transport system. *Magnaporthe oryzae*, the most important rice pathogen, codes for two subfamilies, 7,8-LDS and 10*R*-DOX-epoxyalcohol synthase [7]. The latter also occurs in *Fusarium oxysporum* along with 9*S*-DOX-allene oxide synthase (AOS) [7,8]. Aspergilli express three subfamilies [9]. 5,8-LDS, linoleate 10*R*-DOX, and a third subfamily with only one characterized member so far: (DOX)-9*R*-AOS of *Aspergillus terreus* [10,11]. Mycelia of *A. terreus* oxidize 18:2*n*-6 to 9*R*-HPODE and to an allene oxide [12]. The 9*R*-AOS activities could be linked to a putative DOX-CYP fusion protein,

Abbreviations: AOS, allene oxide synthase(s); CP, chiral phase; COX, cyclooxygenase(s); CYP, cytochrome P450; DiHODE, dihydroxyoctadecadienoic acid; DOX, dioxygenase(s); EAS, epoxyalcohol synthase; 9(10)-EODE, 9(10)-epoxy-10,12(*Z*)-octadecadienoic acid; 9,10-DiHOME, 9,10-dihydroxy-12(*Z*)-octadecamonoenoic acid; 9,14-DiHODE, 9,14-dihydroxy-10(*E*),12(*E*)-octadecadienoic acid; 9-HPODE, 9-hydroperoxy-10(*E*),12(*Z*)-octadecadienoic acid; HPOME, hydroperoxyoctadecamonoenoic acid; HPOTrE, hydroperoxyoctadecatrienoic acid; LDS, linoleate diol synthase; LOX, lipoxygenase(s); NP, normal phase; 10-OPMA, 10-oxophytomonoenoic acid; RP, reversed phase.

* Corresponding author at: Division of Biochemical Pharmacology, Department of Pharmaceutical Biosciences, Uppsala University, Box 591, SE-751 24 Uppsala, Sweden.
E-mail address: Ernst.Oliw@farmbio.uu.se (E.H. Oliw).

http://dx.doi.org/10.1016/j.bbalip.2015.11.009
1388-1981/

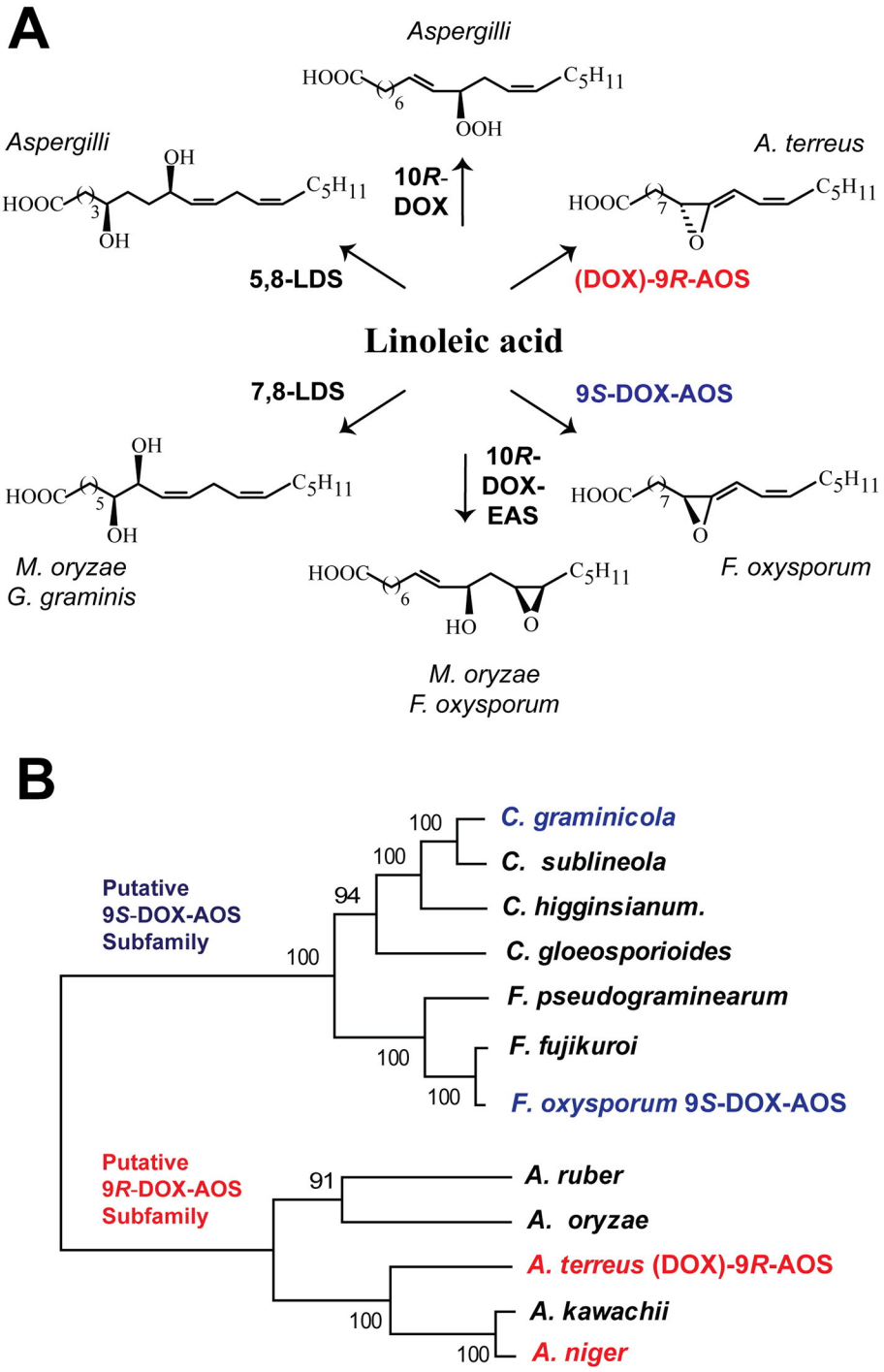

Fig. 1. Overview of fungal oxylipins formed by DOX-CYP fusion enzymes and a phylogenetic tree of homologues to (DOX)-9*R*-AOS of *A. terreus* and 9*S*-DOX-AOS of *F. oxysporum*. A. Linoleic acid is transformed by mycelia and by recombinant enzymes of six subfamilies of DOX-CYP fusion enzymes to diols, epoxy alcohols, allene oxides, and to 10*R*-HPODE. B. A phylogenetic tree of homologues to 9*S*-DOX- and (DOX)-9*R*-AOS, respectively. The tree was generated with MEGA6 [20]. The aligned 9*S*-DOX-AOS protein sequences are from top to bottom: EFQ27323, KDN62523, CCF39565, EQB45385, EKJ79444[2], CCT69067 and EGU88194 (FOXB_01332). The aligned 9*R*-DOX-AOS sequences are EYE96365, BAE60972, AGH14485 (ATEG_02036), GAA91201, and EHA25900. The two enzymes with known catalytic activities are marked, blue for 9*S*-DOX-AOS and red for (DOX)-9*R*-AOS, and the source of the two enzymes studied by recombinant expression is marked in blue and red, respectively. [2]Recombinant expression of EKJ79444 (*F. pseudograminearum*) yielded weak and barely detectable 9-DOX-AOS activities only in a few of several expression experiments. This enzyme was therefore not further investigated (Hoffmann and Oliw, unpublished observation).

AGH14485, by recombinant expression [13], but this fusion protein lacked 9*R*-DOX activities [13]. This could be due to sequencing errors of the tentative 9*R*-DOX domain, but it also raised the possibility that 9*R*-HPODE could be formed by another enzyme [12]. The enzyme is therefore provisionally designated (DOX)-9*R*-AOS until this issue is resolved.

Homologues of (DOX)-9*R*-AOS (AGH14485) with over 62% sequence identities are found in some Aspergilli (Fig. 1B). About 20 homologues with ~50% sequence identities are present in other genera, e.g., Fusarium and Colletotrichum (Fig. 1B) and among them 9*S*-DOX-AOS of *F. oxysporum* [8]. Interestingly, the 9*R*-DOX activities of mycelia of *A. terreus* catalyze suprafacial hydrogen abstraction and oxygen insertion [12], whereas the 9*S*-DOX-AOS of *F. oxysporum* catalyzes antarafacial hydrogen abstraction and oxygenation [8]. This leaves us with two unresolved issues. Do homologues of (DOX)-9*R*-AOS (AGH14485) in Aspergilli possess either 9*R*-DOX and 9*R*-AOS activities or only 9*R*-AOS activities? In the former case, what are the structural

differences between these 9*R*- and 9*S*-DOX domains in regard to the supra- and antarafacial hydrogen abstraction and oxygen insertion?

To answer the first question we decided to recombinantly express the tentative 9*R*-DOX-AOS of *Aspergillus niger* (EHA25900). Regarding the second question, the only characterized enzyme for comparison is 9*S*-DOX-AOS of *F. oxysporum* [8]. We therefore decided to express a second enzyme of the putative 9*S*-DOX-AOS subfamily and we chose *Colletotrichum graminicola* (teleomorph *Glomerella graminicola*). This would allow us to compare two 9*S*-DOX-AOS and their homologues with the putative 9*R*-DOX-AOS subfamily, consisting of EHA25900 (*A. niger*), AGH14485 (*A. terreus*) and homologues of three other Aspergilli. The sequence similarities within and between these two subfamilies are illustrated by a phylogenetic tree (Fig. 1B).

The overall objective of this report was to study the structural basis of the 9*R*- and 9*S*-DOX-AOS activities. The first goal was to determine the catalytic properties of the tentative 9*R*-DOX-AOS (EHA25900) of *A. niger* with homology to (DOX)-9*R*-AOS of *A. terreus*. The second goal was to characterize the tentative 9*S*-DOX-AOS (EFQ27323) of *C. graminicola* with homology to 9*S*-DOX-AOS of *F. oxysporum*. The third goal was to use the sequence information for homologous enzymes to determine whether site-directed mutagenesis of the DOX domains of 9*R*-DOX-AOS could alter the chirality of the hydroperoxide and allene oxide from *R* to *S* at C-9.

2. Materials and methods

2.1. Materials

Fatty acids were dissolved in ethanol and stored in stock solutions (50–100 mM) at −20 °C. 16:3*n*-3 (99%), 18:2*n*-6 (99%), 18:3*n*-6 (99%), and 18:3*n*-3 (99%) were from VWR. 18:1*n*-9, 18:1*n*-6, 20:2*n*-6, and [$^{13}C_{18}$]18:2*n*-6 (98%) were from Larodan (Malmö, Sweden). [11*S*-^{2}H]18:2*n*-6 (>99% ^{2}H) was prepared as described [14]. *S* and *R* stereoisomers of 9- and 13-HPODE were prepared enzymatically or by photooxidation as described [8,15]. Rac 9-HPODE was prepared by autoxidation of linoleic acid followed by purification by reverse phase (RP) and normal phase (NP) HPLC [16]. 9,14-DiHODE was prepared by autoxidation of 18:2*n*-6 as described [17]. [$^{13}C_{18}$]13*S*-HPODE was prepared with soybean LOX (Lipoxidase, Sigma). *Phusion* DNA polymerase and chemically competent *Escherichia coli* (NEB5α) were from New England BioLabs. Restriction enzymes were from New England BioLabs and Fermentas. Champion pET101D Directional TOPO Kit was from Invitrogen. Gel extraction kit and *Pfu* DNA polymerase were from Fermentas. RNaseA, lysozyme, deoxyribonuclease I, and ampicillin were from Sigma. Sequencing was performed at Uppsala Genome Center (BMC, Uppsala University). The open reading frames of EHA25900 (*A. niger*) and EFQ27323 (*C. graminicola*) in pUC57 vectors were ordered from GenScript (Piscataway, NJ 08854). PCR primers were ordered from TIB Molbiol (Berlin, Germany). SepPak columns (silicic acid and C_{18} silica) were from Waters.

2.2. Expression of recombinant proteins

The open reading frames of EHA25900 and EFQ27323 in pUC57 were transferred to pET101D-TOPO vectors by PCR technology according to Invitrogen's instructions. Competent *E. coli* (BL21) Star cells were transformed with the expression constructs by heat shock. Cells were grown until they obtain an A_{600} of 0.6–0.8 in 2xYT medium (Tryptone 16, yeast extract 10 g, NaCl 5 g) at 37 °C (220 rpm) prior to addition of 0.1 mM isopropyl-β-D-galactopyranoside to induce protein expression. After 5 h of moderate shaking (~100 rpm) at room temperature (20 °C), the cells were harvested by centrifugation (13,000 rpm, 4 °C; 25 min), suspended in 50 mM Tris–HCl (pH 7.6)/5 mM EDTA/10% glycerol with lysozyme and deoxyribonuclease I. The suspension was frozen and thawed twice and then sonicated (Bioruptor Next Gen, 10 × 30 s, 4 °C). Cell debris was removed by centrifugation and the supernatants were used immediately or frozen at −80 °C until needed. 9*S*- and 9*R*-DOX-AOS of *A. niger* and *C. graminicola* were expressed in at least three independent expression experiments.

2.3. Site-directed mutagenesis of recombinant proteins

Site-directed mutagenesis was performed according to the QuickChange protocol (Stratagene) with 10 ng of the pUC57 constructs as templates, oligonucleotides (44-nt), and *Pfu* DNA polymerase (16 cycles). PCR products were incubated with DpnI (37 °C, 2 h) to digest methylated DNA. Gel electrophoresis confirmed amplification of one distinct PCR product, which was then used for transformation of *E. coli* (NEB5α) cells by heat shock. All mutations, except for the heme thiolate replacements, were confirmed by sequencing before sub cloning to pET101D-TOPO vectors described above. The Cys1075Ser and Cys1052Ser replacements of EHA25900 and EFQ27323, respectively, were confirmed by expression of recombinant enzyme with abolished 9-AOS but retained 9-DOX activities.

2.4. Enzyme assays

Recombinant proteins of the crude cell lysate (in 0.05 M Tris–HCl (pH 7.6)/5 mM EDTA/10% glycerol) were incubated with 100 μM 18:2*n*-6, other fatty acids, or HPODE for 30–40 min on ice. [11*S*-^{2}H]18:2*n*-6 was only incubated for 10 min and immediately treated with $NaBH_4$ to convert the α-ketol to 9,10-dihydroxy-12(*Z*)-octadecamonoenoic acid (9,10-DiHOME). The reactions (0.3–0.5 ml) were terminated with methanol (1–2 vols.) and proteins were removed by centrifugation. The metabolites were extracted on octadecyl silica (SepPak/C_{18}), eluted with ethyl acetate, evaporated to dryness, diluted in ethanol (50 μl), and 10 μl were subject to LC-MS/MS analysis. Triphenylphosphine or $NaBH_4$ were used to reduce hydroperoxides to alcohols for steric analysis.

2.5. LC-MS analysis

RP-HPLC with MS/MS analysis was performed with a Surveyor MS pump (ThermoFisher) and an octadecyl silica column (5 μm; 2.0 × 150 mm; Phenomenex), which was eluted at 0.3–0.4 ml/min with methanol/water/acetic acid, 750/250/0.05. The effluent was subject to electrospray ionization in a linear ion trap mass spectrometer (LTQ, ThermoFisher). The heated transfer capillary was set at 315 °C, the ion isolation width at 1.5 amu (4 amu for analysis of ^{2} H-labeled metabolites), the collision energy at 35 (arbitrary scale), and the tube lens varied between 90 and 120 V. $PGF_{1\alpha}$ was infused for tuning. Samples were injected manually (Rheodyne 7510) or by an auto sampler (Surveyor Autosampler Plus, ThermoFisher).

NP-HPLC with MS/MS analysis was performed with a silicic acid column (5 μm; Kromasil 100SI, 250 × 2 mm, Dalco Chromtech) using 3% isopropyl alcohol in hexane for separation of oxidized fatty acids (0.3–0.5 ml/min; Constametric 3200 pump, LDC/MiltonRoy). The effluent was combined with isopropyl alcohol/water (3/2; 0.2–0.3 ml/min) from a second pump (Surveyor MS pump; [18]). The combined effluents were introduced by electrospray ionization into the ion trap mass spectrometer above. Chiral phase (CP)-HPLC was performed in the same way. Isomers of 9-HODE were separated by chromatography on Chiralcel OB-H or on Reprosil Chiral-AM. The former was eluted at 0.5 ml/min with hexane/isopropyl alcohol/acetic acid, 95/5/0.01 [19], and mixed post-column with isopropyl alcohol/water (0.25 ml/min). Stereoisomers of α-ketols and 9-HODE were resolved on Reprosil Chiral-AM (5 μm, 250 × 2 mm; Dr. Maisch), eluted at 0.2 ml/min with hexane/ethanol/acetic acid, 95/5/0.025, and mixed with isopropyl alcohol/water (0.15 ml/min).

2.6. Bioinformatics

The ClustalW algorithm was used for sequence alignments (Lasergene, DNASTAR, Inc.). MEGA6 software was used for construction of phylogenetic trees with bootstrap tests of the resulting nodes [20]. SWISS-MODEL was used for alignment and modeling of EHA25900 and EFQ27323 with COX-2 [21]. PyMOL Molecular Graphics System, Version 1.7.4 Schrödinger, LLC, was used for visualization of models.

3. Results

3.1. Expression of EHA25900 (9R-DOX-AOS) and oxygenation of 18:2n-6

MS/MS analysis of mono- and dioxygenated metabolites showed that recombinant EHA25900 oxidized 18:2*n*-6 to a major polar metabolite and to 9-hydroperoxy-10(*E*),12(*Z*)-octadecadienoic acid (9-HPODE) along with variable amounts of epoxyalcohols and diols (Fig. 2A and B). The MS/MS spectrum of the major metabolite was identical with that of an α-ketol, 9-hydroxy-10-oxo-12(*Z*)-octadecenoic acid [12]. Although the α-ketol was a main metabolite in all experiments, we found significant amounts of other polar metabolites, which were derived from 9-HPODE in relatively large amounts in some experiments (peaks I and II in Fig. 2B).

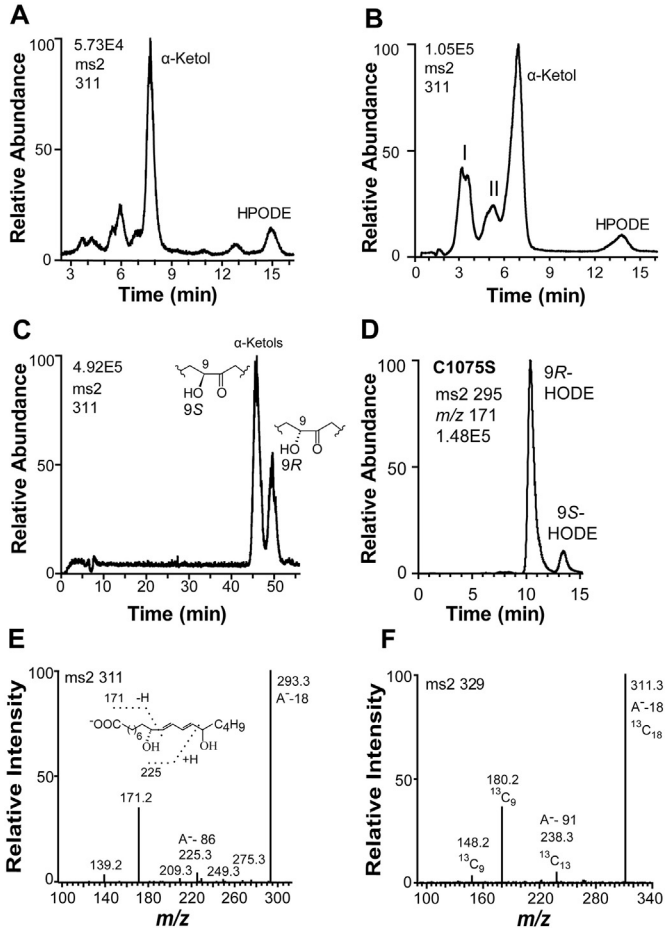

Fig. 2. LC-MS analysis of products formed from 18:2*n*-6 by recombinant EHA25900 (9*R*-DOX-AOS of *A. niger*). A. RP-HPLC-MS/MS analysis of products with molecular mass of 295 and 311. B. The profile of metabolites formed by recombinant EHA25900 varied with an increased formation of polar metabolites in some experiments (peak I, two partly resolved stereoisomers of 9*R*,14(*R*/*S*)-DiHODE; peak II, epoxy alcohols). C. CP-HPLC-MS/MS separation and analysis of the isomers of the α-ketol revealed that the 9*S* stereoisomer was formed in excess, suggesting formation from an allene oxide (9*R*(10)-EODE) by hydrolysis. D. Steric analysis of 9-HPODE formed by the Cys1075Ser mutant of EHA25900 by CP-HPLC-MS/MS (Reprosil Chiral-AM). E. The identical MS/MS spectra (*m*/*z* 311 → full scan) of the two polar metabolites of peak I in B was consistent with isomers of 9,14-DiHODE, likely formed by hydrolysis of 9*R*(10*R*)-epoxy-octadeca-11(*E*),13(*E*)-dienoic acid [23]. F. The identical MS/MS spectra (*m*/*z* 329 → full scan) of the two polar metabolites (cf. peak I in B), which were formed from [$^{13}C_{18}$]18:2*n*-6, was consistent with isomers of [$^{13}C_{18}$]9,14-DiHODE as judged from the number of ^{13}C atoms in the two informative fragments, *m*/*z* 180 (171 + 9) and 238 (225 + 13).

It is well known that non-enzymatic hydrolysis of allene oxides, 9*R*(10)- and 9*S*(10)-epoxy-10,12(*Z*)-octadecadienoic acid (9(10)-EODE), occurs mainly with inversion of configuration at C-9 [22]. The 9*S*- and 9*R*-stereoisomers of the α-ketol were separated by CP-HPLC, and the 9*S*-stereoisomer was formed in excess (65%, Fig. 2C). This suggested that the isomers of the α-ketol were mainly formed from hydrolysis of 9*R*(10)-EODE. To assess the absolute configuration of 9-HPODE formed by the DOX domain, we deleted the AOS activities of EHA25900 by replacement of Cys^{1075} with Ser. Steric analysis showed that this mutant oxidized 18:2*n*-6 to the *R* and *S* stereoisomers of 9-HPODE in a ratio of ~10:1 (Fig. 2D).

The most polar products on RP-HPLC (peak I) were partly resolved (Fig. 2B) and identified as two stereoisomers of 9*R*,14-DiHODE by identical MS/MS spectra. The MS/MS spectra showed characteristic signals at *m*/*z* 171 and 225, which were formed as indicated by the inset in Fig. 2E. This spectrum was identical to that of authentic 9,14-dihydroxy-10(*E*),12(*E*)-octadecadienoic acid (9,14-DiHODE), and the fragmentation was supported by the MS/MS spectrum of the [$^{13}C_{18}$]-labeled metabolite (Fig. 2F). Assuming that the chirality at C-9 is retained, these 9,14-diols are likely formed from hydrolysis of 9(*R*),10(*R*)-epoxy-11(*E*),13(*E*)-octadecadienoate [17,23].

The epoxyalcohols formed from 9-HPODE (*viz.*, 9(10)-epoxy-11-hydroxy- and 9(10)-epoxy-13-hydroxy-octadecenoic acids) eluted between the α-ketol and 9,14-DiHODE (peak II in Fig. 2B). Small amounts of 9-KODE were also detected, but we could not detect formation of 10-oxophytomonoenic acid (10-OPMA).

[11*S*-^{2}H]18:2*n*-6 (99% ^{2}H) was transformed to isomers of the α-ketol (analyzed after reduction of the α-ketol with $NaBH_4$ to 9,10-DiHOME) and 9-HPODE with retention of over 90% of the deuterium label as judged from the signal pairs at *m*/*z* 293/294 ($A^{-}18$) and *m*/*z* 277/278 ($A^{-}18$), respectively. We conclude that 9*R*-DOX-AOS (*A. niger*) mainly catalyzes suprafacial hydrogen abstraction (of the *pro-R* hydrogen) and oxygen insertion.

These experiments showed that EHA25900 possessed dual enzyme activities and it was therefore designated 9*R*-DOX-AOS of *A. niger*. This is the first described 9*R*-DOX-AOS, and its catalytic activities is similar to the enzyme activities of mycelia of *A. terreus* [12].

3.2. Transformation and biosynthesis of hydroperoxides by 9R-DOX-AOS (A. niger)

We next examined the transformation of 9*S*- and 9*R*-HPODE by recombinant EHA25900. 9*R*-HPODE was rapidly consumed by the AOS activities (Fig. 3A). It was transformed to 9(*S*)-hydroxy-10-oxo-12(*Z*)-octadecenoic acid as the main stereoisomer (75%; Fig. 3B). 9*S*-HPODE was also transformed by the AOS activities and converted to 9(*R*)-hydroxy-10-oxo-12(*Z*)-octadecenoic acid as the main stereoisomer (70%; Fig. 3C and D), indicating hydrolysis of an allene oxide, 9*S*(10)-EODE. In addition, significant amounts of epoxyalcohols were also detected by MS^2 analysis (likely 9*S*(10*S*)-epoxy-11-hydroxy- and 9*S*(10*S*)-epoxy-13-hydroxyoctadecenoic acids; data not shown, cf. Ref. [24]).

Incubation of 40 μM rac 9-HPODE with EHA25900 (10 min) transformed about 40% of 9-HPODE by the AOS activities and showed that 9*R*-HPODE was preferentially oxidized (ratio 9*R*:9*S*, 1:2, Fig. 3E, top). The α-ketol of this experiment consisted of the *S* and *R* stereoisomers in a ratio of ~4:3 (Fig. 3E, bottom). We conclude that recombinant EHA25900 was not absolutely specific for the 9*R* stereoisomer of 9-HPODE, but this stereoisomer appeared to be the preferred substrate.

We also assessed the transformation of 13*S*- and 13*R*-HPODE by EHA25900 to allene oxides, but the α-ketol (13-hydroxy-12-oxo-9(*Z*),15(*Z*)-octadecadioenoic acids) formed by non-enzymatic hydrolysis

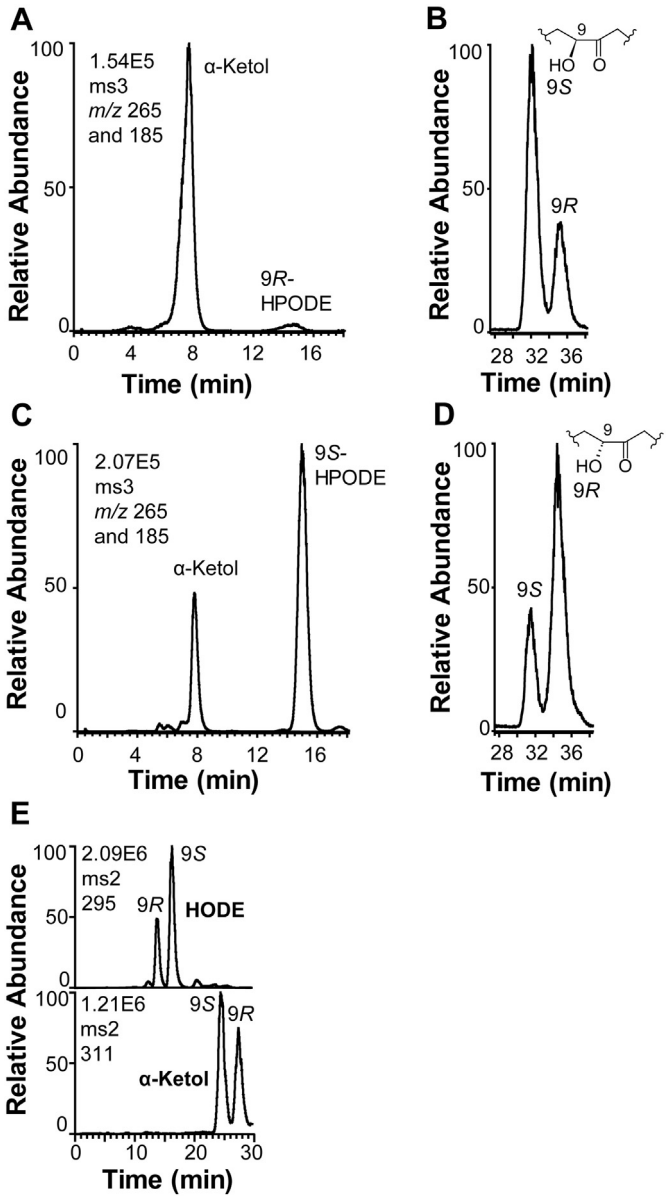

Fig. 3. LC-MS analysis of the α-ketol formed from 9*R*- and 9*S*-HPODE by recombinant EHA25900 (9*R*-DOX-AOS). A. RP-HPLC-MS/MS analysis of products formed from 9*R*-HPODE. B. CP-HPLC analysis and separation of the isomers of the α-ketol formed from 9*R*-HPODE. C. RP-HPLC-MS/MS analysis of products formed from 9*S*-HPODE. D. CP-HPLC analysis and separation of isomers of the α-ketol formed from 9*S*-HPODE. The α-ketol is formed by non-enzymatic hydrolysis of the allene oxide (9*S*(10)-EODE). E. Transformation of *rac* 9-HPODE by EHA25900 and CP-HPLC-MS/MS analysis (Reprosil Chiral-AM) of the stereoisomers of 9-HPODE (top) and the α-ketol (bottom) at the end of the incubation.

of allene oxides could not be detected. 13*S*- and 13*R*-HPODE were both transformed to significant amounts of 12(13)-epoxy-9-hydroxy- and 12(13)-epoxy-11-hydroxyoctadecenoic acids. We conclude that EHA25900 cannot form the allene oxide precursor of jasmonic acid.

3.3. Substrate specificity of 9R-DOX-AOS of A. niger

The 9*R*-DOX activities of 9*R*-DOX-AOS transformed 18:2*n*-6, 18:3*n*-3, and 20:2*n*-6 to hydroperoxides at the *n*-9 positions with 18:2*n*-6 being by far the preferred substrate. The rates of oxidation of 18:3*n*-3 and 20:2*n*-6 to hydroperoxides were only ~16 and ~5%, respectively, of the oxidation rate of 18:2*n*-6 by the Cys1075Ser mutant without AOS activities (designated 9*R*-DOX-AOS•Cys1075Ser and used for quantitation of hydroperoxides). We could not detect any oxidation of 16:3*n*-3, 18:3*n*-6, and 18:1*n*-9 under our experimental conditions. 18:1*n*-6 was transformed to 11-H(P)OME(12*Z*) and 13-H(POME)(11*E*) in a ratio of 5:1 as judged from LC-MS analysis (see Ref. [25] for these MS/MS spectra), but these products were formed in only trace amounts in comparison with metabolites of 18:2*n*-6.

The 9*R*-AOS activities were also restricted. 18:2*n*-6 and 20:2*n*-6, but not 18:3*n*-3, were transformed by the dual enzymatic activities of 9*R*-DOX-AOS. The physiological substrate is therefore likely 18:2*n*-6.

3.4. Expression of EFQ27323 (9S-DOX-AOS) and oxygenation of 18:2n-6

Recombinant EFQ27323 (*C. graminicola*) was expressed to obtain a second enzyme for comparison of 9*S*- and 9*R*-DOX-AOS enzymes. It oxidized 18:2*n*-6 to 9-HPODE and an α-ketol, 9-hydroxy-10-oxo-12(*Z*)-octadecenoic acid, which consistently accumulated as the major metabolite (Fig. 4A). Hydrolysis of an allene oxide, 9*S*(10)-EODE, formed from 9*S*-HPODE, should yield excess of the 9(*R*)-hydroxy-10-oxo-12(*Z*)-octadecenoic acid stereoisomer, and this was also the case (78%; Fig. 4B). Steric analysis of 9-HPODE by CP-HPLC confirmed that the 9*S* stereoisomer was mainly formed (Fig. 4C). This was quantified with aid of the Cys1052Ser mutant without AOS activities. The latter formed over 99% of the *S* stereoisomer.

In addition, several minor metabolites were identified by their MS^2 or MS^3 spectra including the γ-ketol (13-hydroxy-10-oxo-11(*E*)-octadecenoic acids), 9-KODE, and 10-OPMA. The RP-HPLC-MS/MS analysis of the latter two is shown in Fig. 4D.

The MS/MS spectrum of 10-OPMA (*m/z* 293 → full scan) showed, in addition to signals due to losses of H_2O and CO_2, a characteristic signal at *m/z* 177 (90% of the base peak ion at *m/z* 249 (293–44)) and weaker signals at *m/z* 211, 193, and 165 (Fig. 4E). The MS^2 spectrum of the [$^{13}C_{18}$]-labeled metabolite showed that the intense signal at *m/z* 177 was shifted to *m/z* 189 (177 + 12), suggesting an ion with composition of $C_{12}H_{17}O^-$. This MS^2 spectrum was similar to that of the MS^3 spectrum of the γ-ketol [12].

[11*S*-^{2}H]18:2*n*-6 (99% ^{2}H) was transformed to the α-ketol as end product. The α-ketol was analyzed after reduction with $NaBH_4$ to 9,10-DiHOME, which retained the deuterium label with molecular anions at *m/z* 314 (100%) and 313 (<5%). The deuterium label was also retained in 9-HODE as judged from the MS^2 spectrum and the signals due to loss of water from the carboxylate anion ($A^- - 18$) at *m/z* 277 (<10%) and 278 (100%).

We conclude that EFQ27323 possesses dual enzymatic activities. This enzyme was designated 9*S*-DOX-AOS of *C. graminicola*.

3.5. Catalytic properties of 9S-DOX-AOS of C. graminicola

9*S*-HPODE was rapidly and almost completely transformed to the α-ketol, whereas EFQ27323 transformed 9*R*-HPODE somewhat less efficiently. Incubation of EFQ27323 for 10 min with 40 μM rac 9-HPODE converted ~40% of the substrate by the AOS activities and showed that 9*S*-HPODE was preferentially oxidized with a ratio of 9*S*:9*R* of ~1:2. The ratio of the 9*S* and 9*R* stereoisomers of the α-ketol of this experiment was ~2:1. We conclude that 9*S*-HPODE could be transformed about twice as fast as 9*R*-HPODE by EFQ27323.

13*R*- and 13*S*-HPODE were partly converted to epoxyalcohols, but the α-ketol, 13-hydroxy-12-oxo-9(*Z*),15(*Z*)-octadecadienoic acid, could not be detected.

18:3*n*-3 was oxidized to 9-hydroperoxy-10(*E*),12(*Z*),15(*Z*)-octadecatrienoic acid and to an allene oxide, 9(10)-epoxy-10,12(*Z*),15(*Z*)-octadecatrienoic acid, as indicated by the presence of α- and γ-ketols. 20:2*n*-6 was oxidized in analogy with 18:2*n*-6 and 18:3*n*-6 with accumulation of 11-hydroperoxy-12(*E*),14(*Z*)-eicosadienoic acid and an α-ketol, 11-hydroxy-12-oxo-14(*Z*)-eicosenoic acid. 18:2*n*-6 was the preferred substrate. The rates of oxidation of 18:3*n*-3 and 20:2*n*-6 to hydroperoxides were ~48 and ~13%, respectively, of the oxidation rate of 18:2*n*-6 by 9*S*-DOX-AOS•Cys1052Ser (without AOS activities). 18:1*n*-9,

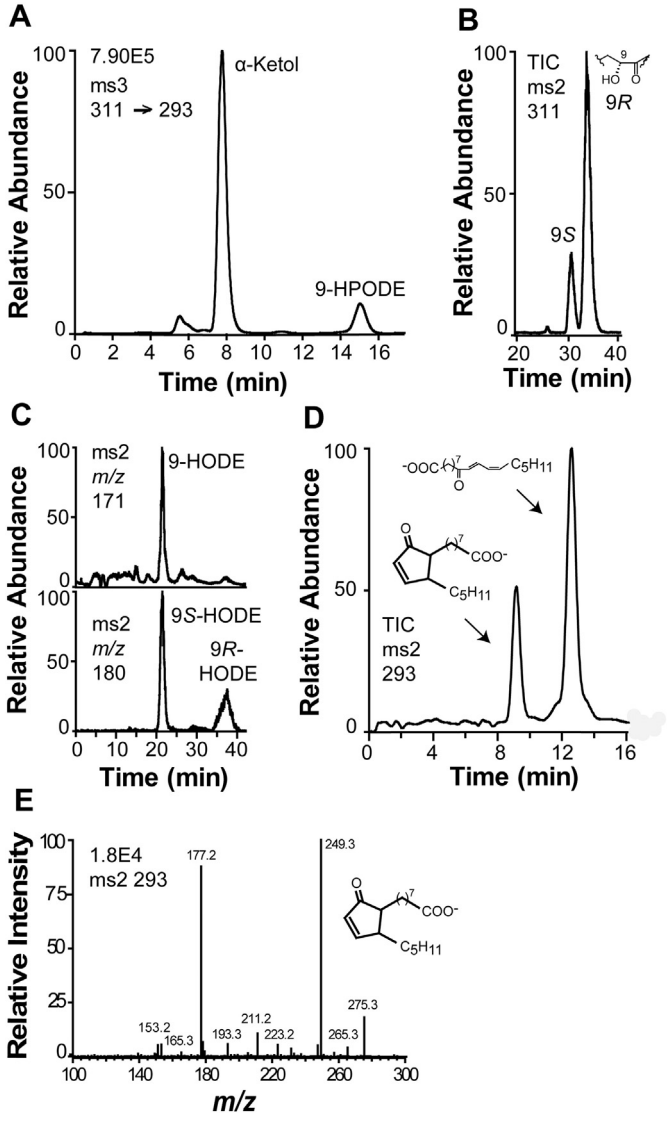

Fig. 4. LC-MS analysis of major products formed from 18:2*n*-6 by EFQ27323 (9*S*-DOX-AOS of *C. graminicola*). A. RP-HPLC-MS^3 analysis (*m/z* 311 → 293 → full scan) revealed that the major product had the same mass spectrum as an α-ketol and the minor product as 9-HPODE. B. Separation of the two stereoisomers of the α-ketol by CP-HPLC-MS/MS analysis. C. CP-HPLC-MS/MS analysis (Chiralcel OB-H) of 9-HPODE after addition of a small amount of racemic [$^{13}C_{18}$]9-HPODE as a marker of the 9*S*- and 9*R*-hydroperoxy stereoisomers. Top chromatogram shows analysis of stereoisomers of 9-HPODE and bottom separation of 9*S* and 9*R* isomers of [$^{13}C_{18}$]9-HPODE. D. LC-MS analysis of two minor products formed from 18:2*n*-6 by EFQ27323 (9*S*-DOX-AOS), namely 10-OPMA and 9-KODE (insets). E. MS^2 spectrum of 10-OPMA with important signals at *m/z* 223 (293–70, possibly loss of C_5H_{10}) and *m/z* 177 (293–44-72; possibly loss of CO_2 and C_5H_{12}).

18:1*n*-6, and 18:3*n*-6 were not converted to significant amounts of products by 9*S*-DOX-AOS under our experimental conditions.

We conclude that 9*S*-DOX-AOS mainly differs from 9*R*-DOX-AOS by oxidation and transformation of 18:3*n*-3 to an allene oxide. It also formed small amounts of 10-OPMA[1].

3.6. Comparison of the amino acid sequences of 9R- and 9S-DOX domains

We compared the alignment of twelve 9-DOX domains, *viz.*, 9*R*-DOX-AOS of *A. niger*, (DOX)-9*R*-AOS of *A. terreus*, three putative 9*R*-DOX-AOS homologues from Aspergilli, 9*S*-DOX-AOS of *F. oxysporum* and *C. graminicola*, and five homologues of 9*S*-DOX-AOS from *Fusarium* and *Colletotrichum*. These twelve sequences formed two distinct branches of the phylogenetic tree (Fig. 1B). We compared the central regions of the 9*S*- and 9*R*-DOX domains (~450 amino acids, from Asn^{248} (*A. niger*) and Asn^{219} (*C. graminicola*) over the distal and proximal heme His ligands to Asn^{680} and Asn^{652}, respectively, at the border of the AOS domains). This revealed >83% amino acid sequence identities within the seven 9*S*-DOX domains and >75% identities within five 9*R*-DOX domain. The sequence identities between 9*S*- and 9*R*-DOX domains were lower but still ranged between 65 to 70%.

The 9*S*- and 9*R*-DOX domains show sequence identities around the distal heme His ligand (Ilelle**His**Asp) and the proximal heme His ligand with the catalytic tyrosine in the characteristic tetramer **Tyr**ArgPhe**His** with Phe in the third position (Fig. 5A). The Phe residue in this position is characteristic of the two 9-DOX-AOS subfamilies, but it is not important for the oxygenation at C-9 [8]. We found 23 conserved amino acid differences between 9*S*- and 9*R*-DOX, marked in red (Fig. 5A), in the central regions of almost 450 amino acids described above. We hypothesized that one of them in particular might contribute to the chirality of 9*R* products.

9*S*- and 9*R*-DOX-AOS catalyze abstraction of the *pro-R* hydrogen at C-11 of 18:2*n*-6, which is followed by antarafacial oxygen insertion by 9*S*-DOX-AOS and by suprafacial insertion by 9*R*-DOX-AOS [8,12]. LOX may bind fatty acids with either the carboxyl group or the ω end embedded at the end of the active site pocket [26,27]. We cannot exclude that the substrate could also be oriented in the opposite orientation in 9*S*- and 9*R*-DOX domains, but this seems unlikely due to the oxygenation of 20:2*n*-6. The oxidation of the latter and 18:2*n*-6 at the *n*-9 positions suggests that both fatty acids enter the active sites with their ω ends. 18:2*n*-6 might be oriented in the same head-to-tail orientation in the 9*S*- and 9*R*-DOX domains, but the oxygen access to C-9 could differ. We therefore compared conserved differences in the twelve 9*S*- and 9*R*-DOX domains, which could explain the *S* and *R* chirality at C-9 of the products.

3.7. Replacement strategy in the 9-DOX domains of 9R- and 9S-DOX-AOS

Hydrophobic residues likely align the active site of the 9-DOX domains. Substitution of Phe with small hydrophobic residues or Ser with Phe may alter the chirality as shown for 13*R*-MnLOX of *Gaeumannomyces graminis* (Phe337Ile) and 11*R*-MnLOX of *F. oxysporum* (Ser348Phe) [19,28]. The Coffa-Brash determinant (Gly/Ala) of the position for oxygenation by 9- and 13-LOX suggests that replacement of Gly residues, which may disrupt α-helices, with Ala or other hydrophobic residues might have profound effects [29]. To reduce the number of candidate amino acids for replacement, we used SWISS MODEL [21] to align and build a model of 9*R*-DOX-AOS with cyclooxygenase-2 (COX-2)(4 ph 9.1.A; 25% amino acid identity) as a template [30]. The goal was to identify amino acid residues likely to be positioned close to the catalytically important Tyr^{441} residue of the active site. This model suggested that Val^{387}, Gly^{397}, and Gly^{616} could be located within ~12 Å and Phe^{627} within ~5 Å from Tyr^{441} (Fig. 5B and C). Based on these considerations, we decided to study the effect of four replacements of 9*R*-DOX-AOS on product chirality: Val387Ile, Gly397Ala, Gly616Ile, and Phe627Leu.

3.8. Phe627Leu replacement of 9R-DOX-AOS (A. niger)

To confirm recombinant protein expression, we verified that the 9*R*-AOS activities were present after replacing Phe^{627} with Leu in the 9*R*-DOX domain. This mutant, designated 9*R*-DOX-AOS•Phe627Leu, almost completely converted 9*R*-HPODE to an α-ketol as the main polar product in analogy with the native enzyme (Fig. 6A).

9*R*-DOX-AOS•Phe627Leu oxidized 18:2*n*-6 to an α-ketol as the main product, but 9-HPODE was also detected. Steric analysis by CP-HPLC showed that 9*S*-HODE was present in larger amounts than 9*R*-HODE and that 9*R* stereoisomer of the α-ketol predominated over the 9*S* stereoisomer (78% R stereoisomer; Fig. 6B). This ratio shows that

[1] 9*S*-DOX-AOS of *F. oxysporum* formed small amounts of 10-OPMA and 9-KODE in the same ratio as 9*S*-DOX-AOS (EFQ27323) of *C. graminicola* (Oliw, unpublished observation).

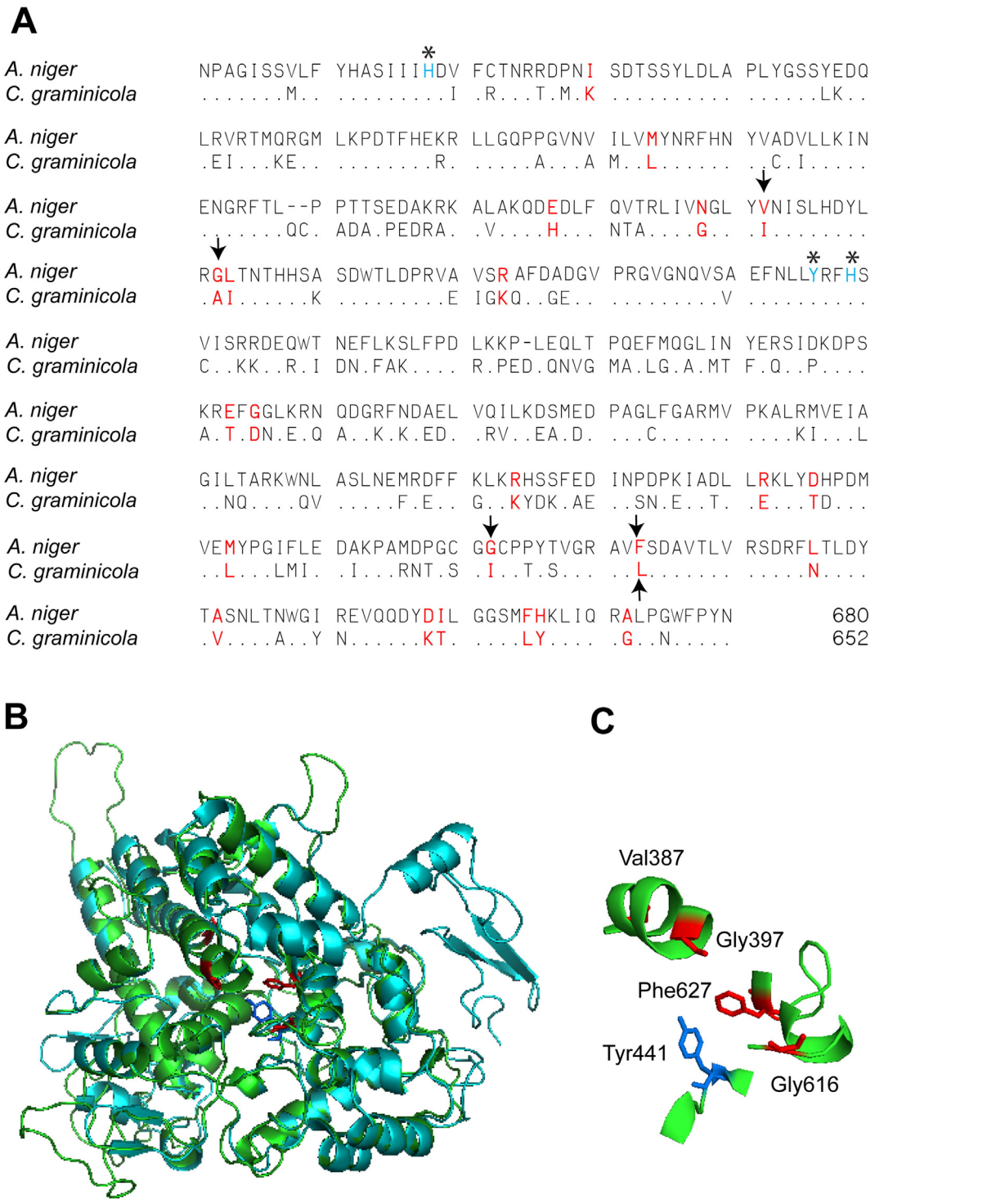

Fig. 5. Partial alignment of the 9-DOX domains of 9*R*-DOX-AOS of *A. niger* and 9*S*-DOX-AOS of *C. graminicola* and a comparison with COX-2. A. The two heme ligands and the catalytically important Tyr residues are marked in blue and the sequence differences in amino acid residues of five 9*R*-DOX-AOS of Aspergilli and seven 9*S*-DOX-AOS of the Fusarium and Colletrotrichum complexes are marked in red (cf. Fig. 1B, where the enzymes are listed). The four residues of 9*R*-DOX-AOS, which are marked with arrows, were investigated by replacements, and so was the marked residue of 9*S*-DOX-AOS (Leu^{601}). The *A. niger* sequence is aligned from Asn^{248} to Asn^{680} and the *C. graminicola* sequence from Asn^{219} to Asn^{652}. B. Model of 9*R*-DOX-AOS (*A. niger*; green) with COX-2 (blue) as a template. C. Overview of four amino acid residues (marked red in B and C; Val^{387}, Gly^{397}, Gly^{616} and Phe^{627}) and the position of Tyr^{441} (marked blue in B and C). Val^{387} is partly hidden by the α-helix.

the α-ketol was mainly formed from 9*S*-HPODE (cf. Fig. 3B). This was validated by analysis of the double mutant, 9*R*-DOX-AOS•Phe627Leu•Cys1075Ser, which was constructed to abolish the AOS activities. The latter formed 9*S*- and 9*R*-HPODE in a ratio of 5:4 (data not shown).

LC-MS analysis confirmed that [11*S*-^{2}H]18:2*n*-6 was oxidized by 9*R*-DOX-AOS•Phe627Leu with retention of the deuterium label in analogy with the 9*R*-DOX activities of mycelia of *A. terreus* and recombinant 9*R*-DOX-AOS (*A. niger*) (Fig. 6C). We conclude that 9*R*-DOX-AOS•Phe627Leu catalyzes antarafacial hydrogen abstraction (of the *pro-R* hydrogen) and

oxygen insertion in analogy with 9*S*-DOX-AOS of *C. graminicola* and *F. oxysporum* [8]. The replacement thus only altered the direction of oxygenation at C-9.

We next examined the importance of the Leu residue by Phe627Ala and Phe627Val replacements. Both mutants showed negligible 9-DOX activities, but the proteins were expressed as judged from transformation of exogenous 9*R*-HPODE to an α-ketol. This illustrates that even small changes of hydrophobic volumes can reduce enzyme activities considerably.

3.9. Gly616Ile, Val387Ile, Gly397Ala and the double mutant Gly616Val/Phe627Leu of 9R-DOX-AOS (A. niger)

9*R*-DOX-AOS•Gly616Ile appeared to slightly increase the relative amounts of 9(*R*)-hydroxy-10-oxo-12(*Z*)-octadecenoic acid and 9*S*-HODE. To validate this observation we incubated 9*R*-DOX-AOS•Gly616Ile with 100 μM [$^{13}C_{18}$]18:2*n*-6 in the presence of 50 μM 9*R*-HPODE to partly quench the AOS activities and increase the 9-HPODE/α-ketol ratio. Analysis of [$^{13}C_{18}$]9-hydroxy-10-oxo-12(*Z*)-octadecenoic acids confirmed an increased biosynthesis of the 9*R* stereoisomer to 44% (Fig. 6D). This was compatible with an increase in the relative formation of [$^{13}C_{18}$]9*S*-HPODE (with a 9*R*-HPODE:9*S*-HPODE ratio of 2:3), but the preferential oxidation of the 9*R* stereoisomer by AOS could lead to overestimation of the 9*S* stereoisomer. We therefore prepared the double mutant of 9*R*-DOX-AOS•Gly616Ile• Cys1075Ser to abolish the AOS activities.

The double mutant formed 9*R*- and 9*S*-HPODE in a ratio of 1:0.3 (insert in Fig. 6D), whereas the single mutant, 9*R*-DOX-AOS•Cys1075Ser, formed these products in a ratio of 1:0.1 (cf. Fig. 2D). We finally examined the triple mutant, 9*R*-DOX-AOS•Gly616Ile•Phe627Leu•Cys1075Ser. This enzyme formed 9-HPODE as the main metabolite and small amounts of epoxyalcohols (Fig. 6E). Steric analysis showed that 9-HPODE consisted of over 90% of the *S* stereoisomer (inset in Fig. 6E). We confirmed that this mutant oxidized [11*S*-^{2}H]18:2*n*-6 with retention of the deuterium label.

9*R*-DOX-AOS•Val387Ile and 9*R*-DOX-AOS•Gly397Ala yielded almost the same relative amounts of the isomers of the α-ketol as formed by native 9*R*-DOX-AOS (Fig. 6F), i.e., about 70% of the *S* stereoisomer of the α-ketol.

3.10. Leu601Phe replacement of 9S-DOX-AOS of C. graminicola

Phe627Leu was found to alter the chirality from 9*R* to 9*S*, and we therefore examined the reverse replacement, Leu601Phe of 9*S*-DOX-AOS (*C. graminicola*). Incubation of 9*S*-DOX-AOS•Leu601Phe with exogenous 9*S*-HPODE led to prominent formation of the α-ketol, but the 9*S*-DOX activities with 18:2*n*-6 was strongly reduced. CP-HPLC analysis of 9-HODE showed that it consisted of the 9*S* stereoisomer. We conclude that other residues than Leu^{601} might be important for the stereospecificity, e.g., Ile^{590} at the homologous position of Gly^{616} of 9*R*-DOX-AOS of *A. niger* (Fig. 5A).

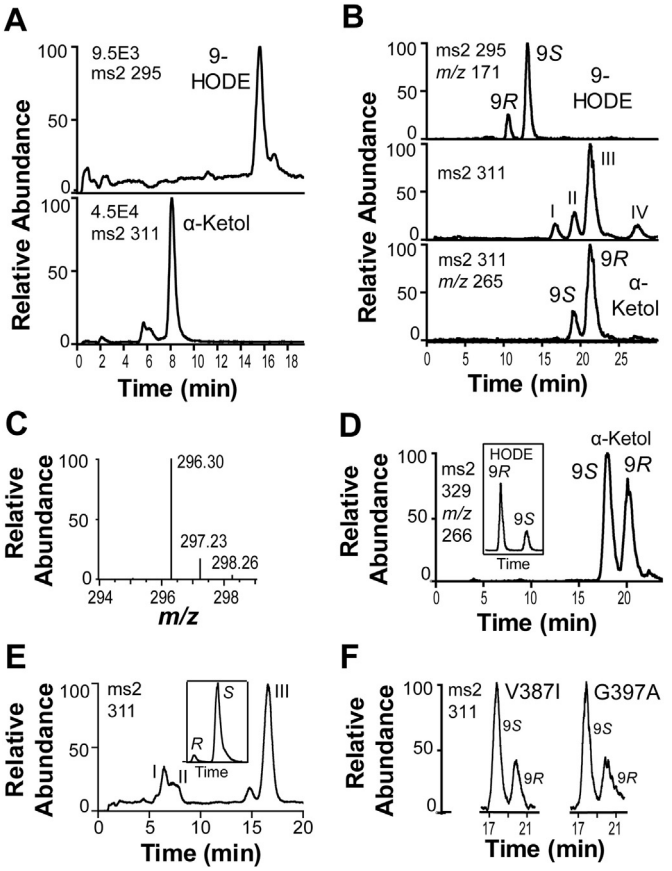

Fig. 6. LC-MS analysis of products formed from 9*R*-HPODE and 18:2*n*-6 by 9*R*-DOX-AOS•Phe627Leu and Gly616Ile. A. RP-HPLC-MS/MS analysis of products formed by 9*R*-DOX-AOS•Phe627Leu from 18:2*n*-6. B. CP-HPLC-MS/MS analysis of the stereoisomers of 9-HODE and the α-ketol formed from 18:2*n*-6 by 9*R*-DOX-AOS•Phe627Leu. The peaks marked II and III in the middle chromatogram contained the stereoisomers of the α-ketol, and peaks I and IV contained epoxy alcohols formed from 9-HPODE. The top chromatogram shows separation of 9R- and 9S-HODE (characteristic ion at *m/z* 171) and the bottom chromatogram shows separation of α-ketols (characteristic ion at *m/z* 265). C. Zoom scan analysis of the carboxylate anion of 9-HODE derived from oxidation of [11*S*-^{2}H]18:2*n*-6 (99% ^{2}H) by 9*R*-DOX-AOS•Phe627Leu. Unlabeled 9-HODE displays a carboxylate anion at *m/z* 295. D. CP-HPLC analysis of the α-ketol formed from [$^{13}C_{18}$]18:2*n*-6 by 9*R*-DOX-AOS•Gly616Ile in the presence of 50 μM 9*R*-HPODE to retard the transformation of [$^{13}C_{18}$]9-HPODE by the 9*R*-AOS activities. [$^{13}C_{18}$]9*S*-HODE was apparently formed in sufficient amounts to increase the formation of the *R* stereoisomer of the [$^{13}C_{18}$]α-ketol. The inset shows the separation of 9*R*- and 9*S*-HODE formed by the double mutant, Gly616Ile/Cys1075Ser, which clearly shows that Gly616Ile increased the relative formation of 9*S*-HPODE (CP-HPLC-MS/MS analysis). E. Analysis of the oxidation of 18:2*n*-6 by the triple mutant, 9*R*-DOX-AOS•Gly616Ile•Phe627Leu•Cys1075Ser, by RP- and CP-HPLC-MS/MS. 9-HPODE was formed as the main product (peak III) along with epoxy alcohols (peaks I and II). The inset shows that 9*S*-HPODE was the main metabolite. The latter was analyzed after reduction to the alcohol (Reprosil Chiral-AM). F. Steric analysis by CP-HPLC-MS/MS analysis of the α-ketol formed from 18:2*n*-6 by the Val387Ile and Gly397Ala mutants of 9*R*-DOX-AOS.

4. Discussion

We have expressed the first 9*R*-DOX-AOS (*A. niger*) with dual enzyme activities, and identified two important amino acid residues for the stereospecificity, Gly^{616} and in particular, Phe^{627}. These Gly and Phe residues are conserved in the 9*R*-DOX-AOS subfamily. Ile^{590} and Leu^{601} are in the homologous positions of 9*S*-DOX-AOS of *C. graminicola*, and these residues are conserved in 9*S*-DOX-AOS subfamily (Fig. 5). The reaction mechanisms of the 9-DOX domains of 9*S*- and 9*R*-DOX-AOS and the single mutant, 9*R*-DOX-AOS•Phe627Leu, are summarized in Fig. 7.

It is well known that amino acid substitutions can alter the position of oxygenation of unsaturated fatty acids by COX and LOX. Replacement of hydrophobic amino acids with smaller or larger residues can alter the position of the fatty acids in the active site, as illustrated by mutagenesis of mammalian COX-1 [31] and by the Sloane, Borngräber, and Coffa-Brash determinants of LOX catalysis [29,32–34]. Replacement with a positively charged residue in the active site of certain LOX can alter the head-to-tail orientation and shift oxygenation from C-13 to C-9 [27]. It is noteworthy that the antarafacial hydrogen abstraction and oxygen insertion are unaffected by these replacements except for oxygen insertion at C-15 of arachidonic acid by COX with 15*R* specificity (*vide infra*) [31,35].

9*R*-DOX-AOS•Phe627Leu altered the absolute configuration of 9-HPODE from mainly 9*R* to mainly 9*S*. Replacement of Gly^{616} with Ile also increased the formation of 9*S*-HPODE and 9*S*(10)-EODE but the effect was less marked. The double mutant, 9*R*-DOX-AOS•Gly616Ile•Phe627Leu, formed over 90% 9*S*-HPODE (Fig. 6E). One possible mechanism is rotation at C-9 after formation of the pentadienyl radical and oxygen insertion as

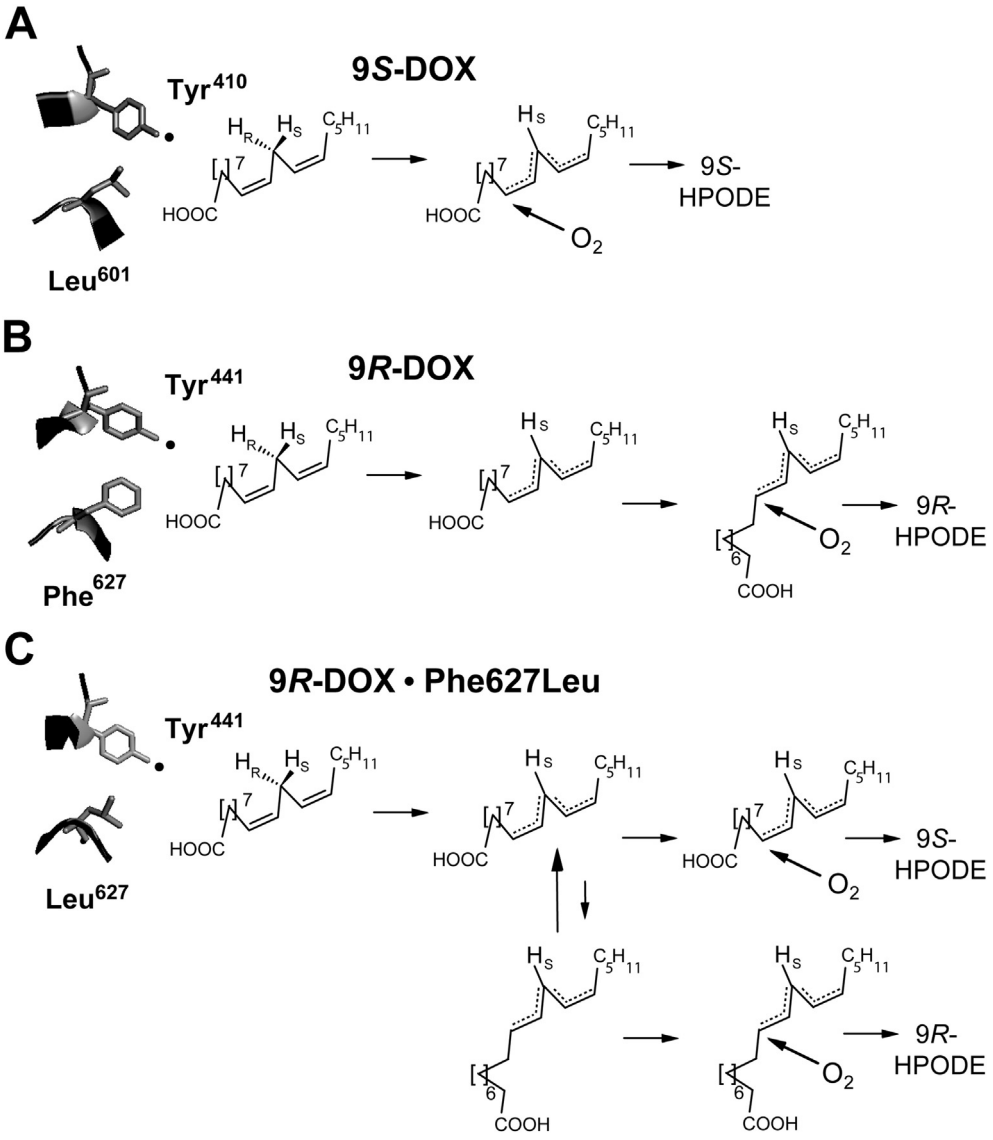

Fig. 7. Schematic overview of the oxidation mechanisms of 9*S*-DOX, 9*R*-DOX and 9*R*-DOX•Phe627Leu. The tyrosyl radicals (marked • on the tyrosine residues) catalyze hydrogen abstraction of the *pro-R* hydrogen at C-11 of 18:2*n*-6. The relative positions of these tyrosine residues and the Leu and Phe residues were obtained by the SWISS-MODEL using murine COX-2 as a template (PDB file 4 ph 9) A. Biosynthesis of 9*S*-HPODE by antarafacial hydrogen abstraction and oxygenation by 9*S*-DOX-AOS. B. Biosynthesis of 9*R*-HPODE by suprafacial hydrogen abstraction and oxygenation, supported by the Phe^{627} residues of 9*R*-DOX-AOS, and a hypothetical rotation at C-9 of the pentadienyl radical after hydrogen abstraction to allow insertion of oxygen from the same side as in A. C. The Phe627Leu mutant of 9*R*-DOX-AOS may bind the substrate in two configurations, one of which favors formation of 9*S*-HPODE, as indicated.

illustrated in Fig. 7. Alternatively, replacement of Phe^{627} with Leu or Gly616 with Ile may alter the direction of oxygen insertion at C-9 from one side to the other (without rotation at C-9).

There is precedence to our observation in the subfamilies of Mn- and Fe-LOX and to some extent, in COX with 15*S*- and 15*R*-specificity. 13*R*-MnLOX of the Take-all fungus of wheat (*G. graminis*) catalyzes suprafacial hydrogen abstraction and oxygenation [36], and this seems to be a common feature of all MnLOX [37]. Replacement of Phe^{337} to Ile in the active site of 13*R*-MnLOX altered the reaction mechanism to mainly antarafacial [19]. This Phe residue is conserved in the MnLOX subfamily and the Ile residues at the homologous position is conserved in all Fe-LOX. COX generally form prostaglandins with *S* configuration at C-15, and 15*S*- and 11*R*-HPETE are also released as side products. There are two exceptions. First, acetylation of Ser^{520} of COX-2 with aspirin abolishes prostaglandin biosynthesis but the acetylated enzyme oxidizes arachidonic acid to 11*R*- and 15*R*-HPETE [38]. Abstraction of the *pro-S* hydrogen at C-13 is retained [38,39]. Second, COX of the coral *Plexaura homomalla* abstracts the *pro-S* hydrogen at C-13, but the end products are prostaglandin endoperoxides with 15*R* configuration along with 15*R*- and 11*R*-HPETE. 15*R*- and 15*S*-specific coral COX can be aligned with 80% sequence identities, and the catalytic difference at C-15 is related to subtle structural differences, e.g., Val or Ile residues at position 349 [35].

The DOX domains of 7,8- and 5,8-DOX-LDS, 10*R*-DOX and 10*R*-DOX-epoxyalcohol synthase catalyze hydrogen abstraction at the allylic position at C-8 by a powerful tyrosine radical [40,41]. These enzymes oxidize 18:1*n*-9 efficiently. It was therefore unexpected that 18:1*n*-9 was a poor substrate of 9*S*-and 9*R*-DOX-AOS. We then hypothesized that a double bond at position n-6 could support hydrogen abstraction at C-11 of C_{18} fatty acids. We thus investigated 18:1*n*-6, but this fatty acid was also a poor substrate of 9*R*- and 9*S*-DOX-AOS. LOX also oxidize 18:1*n*-9 and 18:1*n*-6 at an insignificant rate in comparison with 18:2*n*-6 [25]. We conclude that low rates of oxidation of 18:1 fatty acids cannot be used to differentiate between hydrogen abstraction and oxidation by a catalytic base ($Fe^{3+}OH^{-}$/$Mn^{3+}OH^{-}$) or by a tyrosyl radical.

Interesting questions are the evolution of 9*S*- and 9*R*-DOX-AOS and their biological functions. The signature motifs in the 9-DOX domains are the distal and proximal heme ligands, the catalytically important

Tyr residue, and the Phe/Leu residues important for the direction of oxygen insertion (cf. Fig. 5 and Fig. 7). 9*R*-DOX-AOS are only found in a handful of Aspergilli. Therefore it seems likely that these enzymes have evolved from the 9*S*-DOX-AOS subfamily, which appears to be quite large (Fig. 1A). This transition occurred with relatively few substitutions (Fig. 5A), whereas the 9*R*-AOS domains differ from the 9*S*-AOS domains in a comparatively larger number of amino acid substitutions. These two enzyme oxidize both 9*S*- and 9*R*-HPODE and with only modest stereoselectivity.

The 9-AOS activities catalyze homolytic cleavage of the 9-hydroperoxide with formation of an allene oxide. Asn residues facilitate the biosynthesis of allene oxides by plant AOS (CYP74) [42]. By analogy, Asn, Gln or acid-alcohol residues may assist the homolysis during the fungal biosynthesis of allene oxides [13]. Asn^{964} supports the (DOX)-9*R*-AOS activities [13], but Glu^{946} at the homologous position of 9*S*-DOX-AOS (*F. oxysporum*) had little influence on catalysis [8]. This highlights an unresolved issue: Are there any characteristic structural motives of fungal AOS, e.g., amide amino acids assisting the homolysis of dioxygen bonds by the heme thiolate cysteine in analogy with AOS of plants (CYP74) [42].

5. Conclusion

We have expressed and characterized the first 9*R*-DOX-AOS (*A. niger*) with dual enzyme activities. Sequence homologues are found in *A. terreus* ((DOX)-9*R*-AOS) and a few other Aspergilli. With aid of the 3D structure of COX as a model of the 9*R*-DOX domain and a comparison of twelve 9*R*-DOX-AOS and 9*S*-DOX-AOS sequences we identified by site-directed mutagenesis two important amino acid residues for the 9*R* chirality of the products, Gly^{616} and Phe^{627}.

Conflict of interest

This work was performed without any known conflicts of interest by all participants.

The work consists of traditional academic research without any linkage to industrial or commercial interest, and there are no patent applications based on this work.

Acknowledgements

Supported by Vetenskapsrådet (521-2012-2803), The Knut and Alice Wallenberg Foundation/Grant KAW 2004.0123, and Uppsala University.

References

[1] J.Z. Haeggström, C.D. Funk, Lipoxygenase and leukotriene pathways: biochemistry, biology, and roles in disease, Chem. Rev. 111 (2011) 5866–5898.
[2] A. Andreou, F. Brodhun, I. Feussner, Biosynthesis of oxylipins in non-mammals, Prog. Lipid Res. 48 (2009) 148–170.
[3] A. Andreou, I. Feussner, Lipoxygenases—structure and reaction mechanism, Phytochemistry 70 (2009) 1504–1510.
[4] J. Hansen, A. Garreta, M. Benincasa, M.C. Fuste, M. Busquets, A. Manresa, Bacterial lipoxygenases, a new subfamily of enzymes? A phylogenetic approach, Appl. Microbiol. Biotechnol. 97 (2013) 4737–4747.
[5] W.L. Smith, Y. Urade, P.J. Jakobsson, Enzymes of the cyclooxygenase pathways of prostanoid biosynthesis, Chem. Rev. 111 (2011) 5821–5865.
[6] F. Brodhun, I. Feussner, Oxylipins in fungi, FEBS J. 278 (2011) 1047–1063.
[7] I. Hoffmann, F. Jernerén, E.H. Oliw, Epoxy alcohol synthase of the rice blast fungus represents a novel subfamily of dioxygenase–cytochrome P450 fusion enzymes, J. Lipid Res. 55 (2014) 2113–2123.
[8] I. Hoffmann, E.H. Oliw, Discovery of a linoleate 9S-dioxygenase and an allene oxide synthase in a fusion protein of *Fusarium oxysporum*, J. Lipid Res. 54 (2013) 3471–3480.
[9] J.F. Sanchez, A.D. Somoza, N.P. Keller, C.C. Wang, Advances in aspergillus secondary metabolite research in the post-genomic era, Nat. Prod. Rep. 29 (2012) 351–371.
[10] U. Garscha, E.H. Oliw, Leucine/valine residues direct oxygenation of linoleic acid by (10R)- and (8R)-dioxygenases: expression and site-directed mutagenesis of (10R)-dioxygenase with epoxyalcohol synthase activity, J. Biol. Chem. 284 (2009) 13755–13765.
[11] F. Brodhun, S. Schneider, C. Göbel, E. Hornung, I. Feussner, PpoC from *Aspergillus nidulans* is a fusion protein with one active heme, Biochem. J. 425 (2010) 553–565.
[12] F. Jernerén, I. Hoffmann, E.H. Oliw, Linoleate 9R-dioxygenase and allene oxide synthase activities of *Aspergillus terreus*, Arch. Biochem. Biophys. 495 (2010) 67–73 (Erratum 2010; 500; 210).
[13] I. Hoffmann, F. Jernerén, E.H. Oliw, Expression of fusion proteins of *Aspergillus terreus* reveals a novel allene oxide synthase, J. Biol. Chem. 288 (2013) 11459–11469.
[14] M. Hamberg, Stereochemistry of hydrogen removal during oxygenation of linoleic acid by singlet oxygen and synthesis of 11(S)-deuterium-labeled linoleic acid, Lipids 46 (2011) 201–206.
[15] U. Garscha, T. Nilsson, E.H. Oliw, Enantiomeric separation and analysis of unsaturated hydroperoxy fatty acids by chiral column chromatography-mass spectrometry, J. Chromatogr. B Analyt. Technol. Biomed. Life Sci. 872 (2008) 90–98.
[16] M. Hamberg, Fatty-acid hydroperoxide isomerase in saprolegnia-parasitica—structural studies of epoxy alcohols formed from isomeric hydroperoxyoctadecadienoates, Lipids 24 (1989) 249–255.
[17] M. Hamberg, Autoxidation of linoleic acid. Isolation and structure of four dihydroxyoctadecadienoic acids, Biochim. Biophys. Acta 752 (1983) 353–356.
[18] U. Garscha, F. Jernerén, D. Chung, N.P. Keller, M. Hamberg, E.H. Oliw, Identification of dioxygenases required for aspergillus development. Studies of products, stereochemistry, and the reaction mechanism, J. Biol. Chem. 282 (2007) 34707–34718.
[19] A. Wennman, F. Jernerén, M. Hamberg, E.H. Oliw, Catalytic convergence of manganese and iron lipoxygenases by replacement of a single amino acid, J. Biol. Chem. 287 (2012) 31757–31765.
[20] K. Tamura, G. Stecher, D. Peterson, A. Filipski, S. Kumar, MEGA6: molecular evolutionary genetics analysis version 6.0, Mol. Biol. Evol. 30 (2013) 2725–2729.
[21] M. Biasini, S. Bienert, A. Waterhouse, K. Arnold, G. Studer, T. Schmidt, F. Kiefer, T.G. Cassarino, M. Bertoni, L. Bordoli, T. Schwede, SWISS-MODEL: modelling protein tertiary and quaternary structure using evolutionary information, Nucleic Acids Res. 42 (2014) W252–W258.
[22] M. Hamberg, Mechanism of corn hydroperoxide isomerase: detection of 12(13)-oxido-9(Z),11-octadecadienoic acid, Biochim. Biophys. Acta 920 (1987) 76–84.
[23] K. Niisuke, W.E. Boeglin, J.J. Murray, C. Schneider, A.R. Brash, Biosynthesis of a linoleic acid allylic epoxide: mechanistic comparison with its chemical synthesis and leukotriene A biosynthesis, J. Lipid Res. 50 (2009) 1448–1455.
[24] E.H. Oliw, U. Garscha, T. Nilsson, M. Cristea, Payne rearrangement during analysis of epoxyalcohols of linoleic and alpha-linolenic acids by normal phase liquid chromatography with tandem mass spectrometry, Anal. Biochem. 354 (2006) 111–126.
[25] E.H. Oliw, A. Wennman, I. Hoffmann, U. Garscha, M. Hamberg, F. Jernerén, Stereoselective oxidation of regioisomeric octadecenoic acids by fatty acid dioxygenases, J. Lipid Res. 52 (2011) 1995–2004.
[26] H.W. Gardner, Soybean lipoxygenase-1 enzymically forms both (9S)- and (13S)-hydroperoxides from linoleic acid by a pH-dependent mechanism, Biochim. Biophys. Acta 1001 (1989) 274–281.
[27] E. Hornung, M. Walther, H. Kuhn, I. Feussner, Conversion of cucumber linoleate 13-lipoxygenase to a 9-lipoxygenating species by site-directed mutagenesis, Proc. Natl. Acad. Sci. U. S. A. 96 (1999) 4192–4197.
[28] A. Wennman, A. Magnuson, M. Hamberg, E.H. Oliw, Manganese lipoxygenase of F. oxysporum and the structural basis for biosynthesis of distinct 11-hydroperoxy stereoisomers, J. Lipid Res. 56 (2015) 1606–1615.
[29] G. Coffa, A.R. Brash, A single active site residue directs oxygenation stereospecificity in lipoxygenases: stereocontrol is linked to the position of oxygenation, Proc. Natl. Acad. Sci. U. S. A. 101 (2004) 15579–15584.
[30] B.J. Orlando, M.J. Lucido, M.G. Malkowski, The structure of ibuprofen bound to cyclooxygenase-2, J. Struct. Biol. 189 (2015) 62–66.
[31] E.D. Thuresson, K.M. Lakkides, C.J. Rieke, Y. Sun, B.A. Wingerd, R. Micielli, A.M. Mulichak, M.G. Malkowski, R.M. Garavito, W.L. Smith, Prostaglandin endoperoxide H synthase-1: the functions of cyclooxygenase active site residues in the binding, positioning, and oxygenation of arachidonic acid, J. Biol. Chem. 276 (2001) 10347–10357.
[32] R. Vogel, C. Jansen, J. Roffeis, P. Reddanna, P. Forsell, H.E. Claesson, H. Kuhn, M. Walther, Applicability of the triad concept for the positional specificity of mammalian lipoxygenases, J. Biol. Chem. 285 (2010) 5369–5376.
[33] D.L. Sloane, R. Leung, C.S. Craik, E. Sigal, A primary determinant for lipoxygenase positional specificity, Nature 354 (1991) 149–152.
[34] S. Borngräber, M. Browner, S. Gillmor, C. Gerth, M. Anton, R. Fletterick, H. Kuhn, Shape and specificity in mammalian 15-lipoxygenase active site. The functional interplay of sequence determinants for the reaction specificity, J. Biol. Chem. 274 (1999) 37345–37350.
[35] K. Valmsen, W.E. Boeglin, I. Järving, C. Schneider, K. Varvas, A.R. Brash, N. Samel, Structural and functional comparison of 15S- and 15R-specific cyclooxygenases from the coral *Plexaura homomalla*, Eur. J. Biochem. 271 (2004) 3533–3538.
[36] M. Hamberg, C. Su, E. Oliw, Manganese lipoxygenase. Discovery of a bis-allylic hydroperoxide as product and intermediate in a lipoxygenase reaction, J. Biol. Chem. 273 (1998) 13080–13088.
[37] A. Wennman, E.H. Oliw, Secretion of two novel enzymes, manganese 9S-lipoxygenase and epoxy alcohol synthase, by the rice pathogen *Magnaporthe salvinii*, J. Lipid Res. 54 (2013) 762–775.
[38] G. Xiao, A.L. Tsai, G. Palmer, W.C. Boyar, P.J. Marshall, R.J. Kulmacz, Analysis of hydroperoxide-induced tyrosyl radicals and lipoxygenase activity in aspirin-treated human prostaglandin H synthase-2, Biochemistry 36 (1997) 1836–1845.
[39] C. Schneider, A.R. Brash, Stereospecificity of hydrogen abstraction in the conversion of arachidonic acid to 15R-HETE by aspirin-treated cyclooxygenase-2. Implications for the alignment of substrate in the active site, J. Biol. Chem. 275 (2000) 4743–4746.

[40] C. Su, M. Sahlin, E.H. Oliw, A protein radical and ferryl intermediates are generated by linoleate diol synthase, a ferric hemeprotein with dioxygenase and hydroperoxide isomerase activities, J. Biol. Chem. 273 (1998) 20744–20751.
[41] A.J. Fielding, F. Brodhun, C. Koch, R. Pievo, V. Denysenkov, I. Feussner, M. Bennati, Multifrequency electron paramagnetic resonance characterization of PpoA, a CYP450 fusion protein that catalyzes fatty acid dioxygenation, J. Am. Chem. Soc. 133 (2011) 9052–9062.
[42] D.S. Lee, P. Nioche, M. Hamberg, C.S. Raman, Structural insights into the evolutionary paths of oxylipin biosynthetic enzymes, Nature 455 (2008) 363–368.